

# ALTERNATIVE SOLUTION BY ORTHOGONAL COLLOCATION IN THE REGENERATION SYSTEM

L. M. F. LONA BATISTA and R. MACIEL FILHO

*Univer. Estadual de Campinas - Fac. Eng. Química - Dep. Processos Químicos*  
Campinas, SP, Brazil, CEP 13081-970 - CX postal 6066, email: liliane@feq.unicamp.br

KEYWORDS: Orthogonal Collocation, Regeneration System, Modelling and Simulation

## 1. INTRODUCTION

Orthogonal collocation (OC) methods have been used in many chemical engineering problems such as calculation of effectiveness factors, packed bed analyses and fluid flow problems. In Finlayson (1971), the equations governing a packed bed reactor with radial temperature and concentration gradients are solved using the OC method. The method is shown to be faster and more accurate than finite difference calculations.

In this work, an industrial catalytic cracking regeneration system was simulated. The model equations form a system of non linear integro differential equations. In Maciel Filho *et al.* (1996), the Runge Kutta (RK) method and Trapezoidal Rule are used to solve the model equations, but in this present work, OC method is adopted. Generally, integrals calculation by quadrature is not made simultaneously with differential and algebraic equation, but in this work, this is the case. So, a new methodology is proposed to solve the integrals, based on an approximation of quadrature formula. The simulation results obtained through OC and RK are compared with industrial data from Petrobrás (Brazilian Oil Company).

## 2. PROCESS DESCRIPTION

The diagram for the catalytic cracking industrial unit is depicted in Figure 1. Deactivated catalyst flows from catalytic cracking reactor (CCR) into regeneration system, composed by fluidized bed reactor (FBR) followed by riser (R) and freeboard (FR). The fluidized bed consists on jet and bubble bed zones. The jet region is idealised as a fully mixed zone, as can be seen in Maciel *et al.* (1996). In the riser exit, the solid flow is divided in such way that part of particle goes to freeboard and part returns to tank A, with solids collected by cyclones. A certain amount of catalyst present in vase A returns to bubble bed, and the rest is transported to the cracking reactor.

## 3. ORTHOGONAL COLLOCATION ON REGENERATION SYSTEM SIMULATION

First, the riser and freeboard are simulated, and latter, the fluidized bed reactor. In this last reactor, the bed is split into jet and bubbling phase (Maciel Filho *et al.*, 1996). It was assumed C, H and CO combustion. Details about kinetic parameters can be seen in Maciel *et al.* (1996).

### 3.1 Orthogonal Collocation on Riser and Freeboard

It is assumed PFR heterogeneous model to simulate these both reactors. The model equations form a system of ordinary differential equations, which can be seen in Maciel Filho and Lona Batista (1995). When OC method is adopted, a discretized equation system is generated. The material balances are formulated for solid compounds (Carbon and Hydrogen), as well as for the four gaseous compounds *i* (O<sub>2</sub>, CO, CO<sub>2</sub>, H<sub>2</sub>O). Thus, the following equations can be written:

$$\text{gas compound } i : \quad \sum_p^{N+2} A_{jp} C_{Rj} = \frac{\sum_m K'_{\text{car}}(x_j) \times (1 - E_j) + \sum_l K'_{\text{ox}}(x_j) \times E_j}{U_{\text{tr}}}$$

$$\text{carbon balance:} \quad \sum_p^{N+2} A_{jp} C_{Cp} = \frac{K'_{\text{car,bub}}(x_j) \times PM_{\text{car}} \times (1 - E_j) \times A_R}{Q_{\text{tr}}}$$

$$\text{hydrogen balance:} \quad \sum_p^{N+2} A_{jp} C_{Hp} = \frac{K'_{\text{hd,bub}}(x_j) \times PM_{\text{hd}} \times (1 - E_j) \times A_R}{Q_{\text{tr}}}$$

$$\text{solid phase thermal balance:} \quad \rho_s C_p v_s \left( \sum_p^{N+2} A_{jp} T_{sp} \right) = \sum_m K'_{\text{car}}(x_j) \times (-\Delta H_{R,m})_j - h a_s (T_j - T_{\text{tr}})$$

$$\text{gas phase thermal balance:} \quad \frac{Q_{\text{tr}} C_{p,g}}{A} \left( \sum_p^{N+2} A_{jp} T_{sp} \right) = h a_s (T_j - T_{\text{tr}}) f_s + K'_{\text{bun}}(x_j) \times (-\Delta H_{R,i})_j$$

Figure 2 shows O<sub>2</sub> profiles along the riser, when RK and OC with 4 internal collocation points (ICP) are considered. It can be noticed an agreement in results. This behaviour is also observed in the freeboard (not shown).

### 3.2 Comparison between the Broyden and Newton

The algebraic equation system presented is solved using 2 different procedures. Initially, the Newton method is used to linearize the equations, that are solved by LU decomposition method, latter, the Broyden method is also adopted.

Figure 3 depicts gas temperature profile along riser length. For the OC method, it is assumed 1 and 2 ICP. Newton and Broyden methods are used to solve algebraic equations when 1 ICP is adopted. It can be concluded that Broyden and Newton method present similar accuracy, but the first one is more efficient. When it is assumed error lower than  $10^{-8}$ , the convergence is achieved after 15 iterations to the Newton method and after 5 iterations to the Broyden method. So, Broyden method will be adopted in this work.

### 3.3. Orthogonal Collocation on the Fully Mixed Zone

The system of equations that models the fully mixed zone in the fluidized bed can be seen in Maciel *et al.* (1996). When OC is applied, the differential equations are discretized, and the algebraic equations remain unchanged.

$$\begin{aligned}
 \text{gas compound } i: & \quad \frac{F_i R}{P} (T_0 C_{0,i} - T_{FMZ} C_{FMZ,i}) = \sum_k K_{FMZ,i} \\
 \text{carbon balance:} & \quad V_s (C_{C_0} - C_{C_{FMZ,j}}) = K_{cor,FMZ} (x_j) PM_{cor} \\
 \text{hydrogen balance:} & \quad V_s (Ch_0 - Ch_{FMZ,j}) = K_{hd,FMZ} (x_j) PM_{hd} \\
 \text{solid phase energy balance:} & \quad \rho_s C_p V_s \left( \sum_p A_{jp} T_{s,p} \right) = \sum_m K_{hd,m}^d (x_j) \times (\Delta H_{R,m})_j - h(T_{s_j} - T_{g_j}) \alpha_s \\
 \text{gas phase energy balance:} & \quad \frac{Q_g C_p V_g}{A} \left( \sum_p A_{jp} T_{g,p} \right) = h \alpha_s (T_{s_j} - T_{g_j}) \beta + K_{tmax}^d (x_j) \times (-\Delta H_{R,i})_j
 \end{aligned}$$

The generated profiles from RK and OC method are divergent (Figure 4). As greater is the number of collocation point, more accurate are the results, but the same results are obtained when 4 or 5 points are used. This means that 4 points are enough.

The divergence between RK and OC method occurs due to the presence of algebraic equations. In the methodology presented in Maciel Filho and Lona Batista (1995) to solve the system of equation through RK method, the inlet condition for the second integration step represents the exit condition for the first one. Algebraic equations idealise perfectly mixed behaviour, and differential equations represent plug flow. When RK method is applied, the algebraic equations are solved in a sequential way, so it is assumed several CSTRs, and consequently a PFR behaviour. On the other hand, when OC is used, the model equations are solved simultaneously for all collocation points, so the algebraic equations always represent perfectly mixed behaviour. The inlet concentration or temperature are always assumed in  $x = 0$ . In Figure 5, the jet region is splitted of into 2, 4 and 40 sections, and each of them is solved through OC method. This approach tries imitate the methodology applied in the RK method. As greater is the number of sections, closer are the profiles obtained via RK and OC. When there is division on jet phase,  $C_{co}$  represents the carbon concentration in the exit of previous section, similarly to the RK methodology.

### 3.4. Orthogonal Collocation in the Bubbling Bed

The equation system generated from heterogeneous modelling of bubbling bed can be seen in Maciel *et al.* (1996). When OC method is adopted the equation system become:

#### Gas compound i, emulsion phase

$$\sum_k K_{B,i} (x_j) = \frac{F_B R}{P} (T_{FMZ} C_{FMZ,i} - T_{D_j} C_{B,i,j}) + \frac{F_B K_{be} R T_{D_j}}{U_B P} \left( \sum_j w_j C_{B,i,j} - \sum_j w_j C_{E,i,j} \right) \quad (1)$$

$$\text{Gas compound } i, \text{ bubbling bed:} \quad \sum_{p=1}^{N+2} A_{jp} C_{B,i,p} = -\frac{K_{be}}{U_B} (C_{B,i,j} - C_{E,i,j}) + \frac{\sum_k K_{B,i} (x_j)}{U_B}$$

$$\text{Carbon balance:} \quad V_s (C_{C_{FMZ}} - C_{C_{B,j}}) = K_{cor,B} (x_j) PM_{cor}$$

$$\text{Hydrogen balance:} \quad V_s (Ch_{FMZ} - Ch_{B,j}) = K_{hd,B} (x_j) PM_{hd}$$

$$\text{Solid phase Thermal balance:} \quad \rho_s C_p V_s \left( \sum_p A_{jp} T_{s,p} \right) = \sum_m K_{hd,m}^d (x_j) \times (\Delta H_{R,m})_j - h(T_{s_j} - T_{g_j}) \alpha_s$$

$$\text{Gas Phase Thermal balance:} \quad \frac{Q_g C_p V_g}{A} \left( \sum_p A_{jp} T_{g,p} \right) = h \alpha_s (T_{s_j} - T_{g_j}) \beta + K_{tmax}^d (x_j) \times (-\Delta H_{R,i})_j$$

$$\text{Eq. (1) in its original form is:} \quad \sum_k K_{B,i} = \frac{F_B R}{P} (T_{FMZ} C_{FMZ,i} - T_{D_j} C_{B,i,j}) + \frac{F_B K_{be} R T_{D_j}}{U_B P} \int_{h_j}^H (C_{B,i} - C_{E,i}) dx$$

The integral limits  $h_j$  and  $H$  must be normalised between 0 and 1 before applying quadrature formula. Initially, it was assumed that fluidized bed length is 1 m. By simplicity, it was considered

initially only one ICP. So, concentration and temperature must be calculated on  $x = 0.5\text{ m}$  and  $x = 1\text{ m}$  (the inlet conditions are known).

When equations are solved at  $x = 0.5\text{ m}$ , the integral in the emulsion phase balance have limits 0 and 0.5. By quadrature formula it can be written:

$$\int_0^{0.5} W(x)y(x)dx = \sum_{i=1}^N y_i w_i$$

After changing integral limits from 0 - 0.5 to 0 - 1, another problem is found. When the calculations are made in the bed centre, it is necessary to know the concentration in bubble and emulsion phase at point  $x = 0.25$ , in order to solve the integrals by quadrature. Meanwhile, these concentrations are unknown.

So, in this work, it is developed an approach to resolve this problem. For that, it is considered that the integral of a function between 0 and  $r$  is equal to the product between  $r$  (root of Jacobi polynomial) and integral of function over limits 0 and 1. So, if it is considered  $W(x) = 1$ , we have:

$$\int_0^r y(x)dx = r \int_0^1 y(x)dx \quad (2)$$

As smaller is the variation of function with the co-ordinate ( $x$ ), more real is this approach. For constant functions this is really true.

It can be noticed that RK and OC method promote similar results along 1 m of bed (not shown). Figure 6 shows that carbon monoxide concentration profiles from RK and OC method are different when the simulation is made considering all length of fluidized bed. The approach expressed in equation (2), in this case, is less accurate because the bed is longer.

The bubbling bed simulation was made assuming that the bed is composed of sections of 1 m each. The results are shown in Figure 7. It can be noticed that the profiles obtained from RK and OC are more similar (this behaviour was also observed when the jet region was sectioned).

In this work, it is also proposed a second approach to calculate the integral in the internal collocation points based on the quadrature formula. It can be written that:

$$\int_0^1 y(x)dx = \sum_{i=1}^N y_i w_i \quad (3)$$

If it is assumed 5 collocation points, this integral can be expressed by summation of 5 terms:

$$\int_0^1 y(x)dx = w_1 y(r_1) + w_2 y(r_2) + w_3 y(r_3) + w_4 y(r_4) + w_5 y(r_5)$$

where:  $r_2, r_3, r_4$  are roots in the internal collocation points,  $r_1 = 0$  and  $r_5 = 1$ .

In this second approach, it is assumed that integral between 0 and  $r_p$  may be approximate by:

$$\int_0^{r_p} y(x)dx = \sum_{i=1}^p y_i w_i \quad (4) \quad \text{where: } p = \text{collocation point and } r_p = \text{root in point } p$$

Expression (4) is true for  $r_p = 0$  and  $r_p = 1$ , and it represents an approximation for ICP. Table 1 shows the equation (4) applied in the integral calculation for the function  $f(x) = 5x$  (function arbitrarily chosen). It is obtained better results when  $r_p$  is close to 1.

Figure 8 shows the results using this second approach. The concentration profiles in the emulsion phase become oscillatory. This oscillation is due to inaccuracy in equation (4), mainly when integrals are calculated near root 0. So, in bubbling bed simulation it was used the first approach (equation 2), and the bed was divided in sections of 1 m each.

#### 4. MODELLING APPLIED TO THE INDUSTRIAL SYSTEM

Operation conditions and dimensions for the regeneration system are shown in Tables 2 and 3 respectively. In order to verify if equation (2) is accurate to represent the integral when the superior limit is a ICP, a test is proposed. The bubble region is divided into sections of 1 m each. In order to facilitate the calculations, it is used only one ICP for each section. Simulations using 1, 2 or 3 ICP are made, but they indicate that there are no appreciable divergence in results (not shown), so this hypothesis does not represent limitation in this test.

In this procedure, initially, the integral in  $x = 0.5$  is calculated according to equation 2. After solution of material and energy equations, concentration and temperature are obtained in the collocation points. The interpolation is done, and concentration and temperature in  $x = 0.25$  are obtained. With the emulsion and bubble phase gas concentration at  $x = 0.5$  and  $0.25$ , the integrals may be calculated in an exact way. So, the values of integrals are compared with that obtained in the last iteration. If difference between them are greater than the allowed error, the actual integral calculation is used to determine concentration and temperature profiles.

This procedure is repeated until the difference in the integral calculation between 2 consecutive iteration does not exceed the allowed error.

By using this procedure, concentration and temperature profiles are obtained. These results are compared with that obtained when only equation (2) is used to calculate the integrals in the internal collocation points. It can be noticed that the profiles are coincident (not shown). So, the approach represented by equation 2 is adequate when the model equations are calculated for a specific length of the bubble bed. Figure 9 shows the gas compounds profiles in dry base obtained

from RK and OC methods, and Figure 10 presents the solid temperature profiles. The industrial data are also shown. Through these figures it can be noticed that the second method is more adequate to simulate the industrial regeneration system.

## 5. CONCLUSIONS

In this work, an alternative solution methodology based on OC, was adopted to simulate an industrial catalytic cracking regeneration system.

Concentration and temperature profiles from RK and OC method present different behaviours if there exist algebraic equation in the equation system. In the OC method, algebraic equation represents a perfectly mixed behaviour. In the methodology presented by Maciel *et al.* (1996), algebraic equations represent a sequence of perfectly mixed cells, when RK is adopted.

In the bubble bed simulation, the equation system presents integrals. When the integration is made in internal collocation points ( $r$ ), it is proposed an approach at which the integral between 0 and  $r$  is equal the integral between 0 and 1 multiplied by root of Jacobi polynomial. It is observed that when this approach is used, the results are the same to that obtained if integral calculation is carried out.

Comparison with industrial data shows that RK method can predict well the concentration values, meanwhile the temperatures stay subpredicted. It can be noticed that OC is adequate in simulation of regeneration system, and the results agree with industrial data from Petrobrás. The bubble region of fluidized bed was divided in sections of 1 m each during simulation. This height can be used as an adjustable parameter of model in order to solve industrial problems.

*Acknowledgements* – The authors thank the industrial data provided by Petrobrás.

## NOTATION

A = area of the reactor,  $m^2$ , matrix elements  
 $a_v$  = interfacial area gas-solid,  $l/m$   
 C = gas molar concentration,  $kmol/m^3$   
 Cc = carbon concentration, kg carb/kg catal  
 Ch = hydrogen concentration, kg hyd / kg cat  
 Cp = specific heat,  $kJ/kg K$   
 E = porosity of the bed  
 fs = volumetric fraction of solid  
 H,  $h_j$  = bed height, jet height (m)  
 h = heat transfer coefficient  $kJ/K s m^2$   
 $k_{be}$  = bubble-emulsion mass transfer coefficient  
 K = reaction rate group,  $kmol/s$   
 $K'$  = reaction rate group,  $kmol/s m^3_p$   
 $K''$  = reaction rate group,  $kmol/m_p^3 s$   
 P, PM = pressure, atm; molecular weight

Q = mass flow rate,  $kg/s$   
 R = ideal gas constant  
 T = temperature, K  
 U = superficial velocity,  $m/s$   
 $\Delta H$  = reaction heat,  $kJ/kmol$   
 $\rho$  = specific mass,  $kg/m^3$   
*indices*  
 0 = initial  
 B, car = bubble, carbon phase  
 E, D = emulsion, dense phase  
 FMZ, g = fully mixed zone, gas phase  
 het, hid, hom = heterogeneous, hydrogen, homogeneous  
 i, l, m = gas component, reaction  $l$ ,  $m$   
 R, s, t = riser, solid phase, total

## REFERENCES

- Finlayson, B. A., Chem. Eng. Sci., V. 26, pp. 1081-1091 (1971).  
 Maciel Filho R. and Lona Batista L. M. F., Modelagem Heterogênea de Regeneradores Industriais Considerando a Recirculação de Sólidos", *Anais do Iberian Latin American Conference on Computational Methods for Engineering*. (1995)  
 Maciel Filho R., Lona Batista L. M. F., Mozart Fusco, *Chem. Eng. Sci.*, Vol. 51, N. 10 (1996)

## TABLES AND FIGURES

Table 1: Analyses of the second approach

roots	$\int_0^1 f(x)$	
	analytic results	approach (4)
$r_1 = 0$	0	0
$r_2 = 0.1127$	0.03175	0.1677
$r_3 = 0.5$	0.625	0.6438
$r_4 = 0.8873$	1.968	1.964
$r_5 = 1$	2.5	2.5

Table 3: Dimension of regeneration system

Section / Dimension	Length (m)	Diameter (m)
Combustor	6.71	5.18
Riser	20.09	2.74
Freeboard	8.12	7.67

Table 2: Operation data to regeneration

Variable / case	I	II
Air flow rate (kg/s)	28.08	25.3
Catalyst flow rate (kg/s)	326.5	307.
Recirculation (kg/s)	107.8	225.
Pressure (atm)	2.88	2.65
Retificator temperature (K)	534	560
Air regeneration temperature (K)	217	202
Coke in catalyst (% weight)	0.78	0.60
H / Coke (% weight)	7.5	4.50

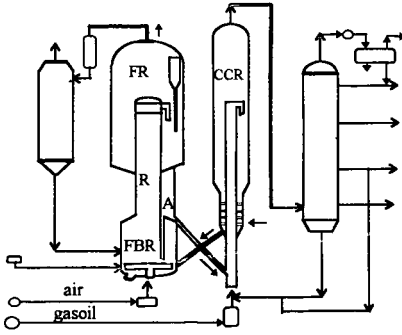


Figure 1: Diagram for a catalytic cracking industrial unit

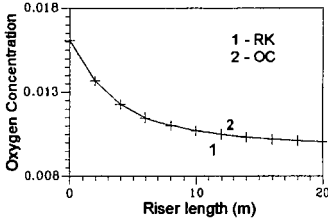


Figure 2: Oxygen Profiles

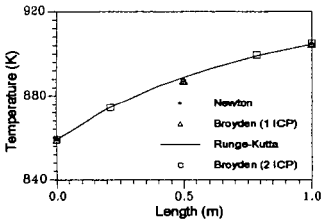


Figure 3: Gas temperature profile.

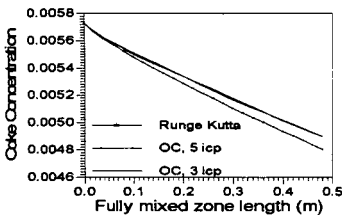


Figure 4: Carbon profiles

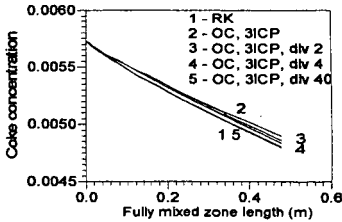


Figure 5: Carbon profiles in jets.

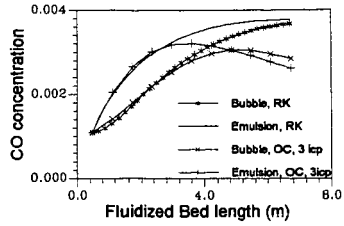


Figure 6: CO profile along bubbling bed

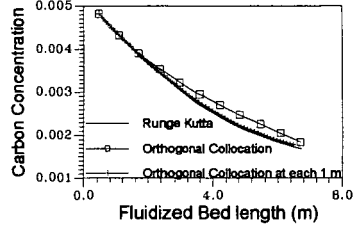


Figure 7: Carbon profile

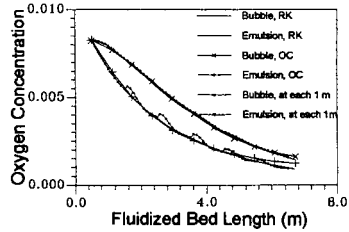


Figure 8: Oxygen profile

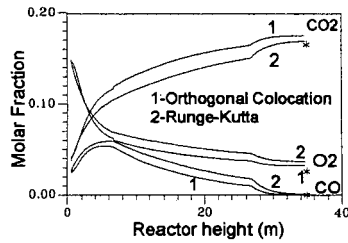


Figure 9: Gas molar fraction

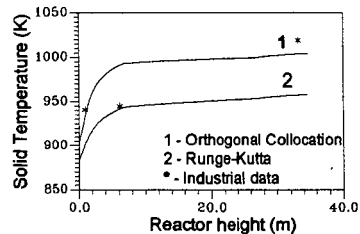


Figure 10: Solid temperature profiles